Prussian Blue Analogues Cubes in the Organic Polymer Electrospun Fibres

A. Pacanowska[a], N.K. Chogondahalli Muniraju[a],
W. Sas[a,b], M. Perzanowski[a],
M. Mitura-Nowak[a] and M. Fitta[a]

[a]*Institute of Nuclear Physics Polish Academy of Sciences, Radzikowskiego 152, 31-342 Kraków, Poland*
[b]*Institute of Physics, Bijenička 46, 10000 Zagreb, Croatia*

This report presents the preparation and characterization of a new composite containing Prussian blue analogues nanoparticles and poly(N-vinyl-2-pyrrolidone) (PVP). Nanoparticles of nickel hexacyanoferrate (NiHCFe) and nickel hexacyanochromate (NiHCCr) were synthesized by the citrate-assisted co-precipitation method. Basic characterization revealed uniform cubic particles with an average size of 238 nm (NiHCFe) and 80 nm (NiHCCr). In the next step, these nanocubes were incorporated into composite fibres using electrospinning technique. The resulting fibres exhibited distinctive colours, and scanning electron microscope imaging showed differences in fibre morphology between NiHCFe/PVP and NiHCCr/PVP composites. The obtained results indicate the successful synthesis and characterization of Prussian blue analogue nanoparticles, as well as their integration into composite fibres, opening up possibilities for diverse applications.

topics: molecular magnetism, Prussian blue analogues, nanoparticles, electrospun fibres

1. Introduction

Prussian blue analogues (PBAs) are examples of compounds showing unique properties, e.g., room temperature ferromagnetism, compensation point, or zero thermal expansion [1–4]. Moreover, PBAs are examples of mixed-valence compounds due to the metal-to-metal charge transfer mediated by the cyano ligand and possess structural flexibility due to the stretching and vibrational modes of the cyano-bridging ligand [5]. These features play important roles in the various magnetic functionalities, such as reversible photomagnetism, humidity-sensitive magnetism, or high ionic conductivity [6, 7]. The attributes described above make these materials useful in practical applications, including gas storage, catalysis, batteries, and energy separation. Prussian blue (PB) and PBAs are also the subjects of increasing interest because of the possibility of producing molecule-based magnets in reduced dimensionality, i.e., in thin films and nanoparticles [8]. Easy synthesis route, controllable shape and size, biocompatibility, biodegradability, and low production cost make the PB/PBA nanoparticles suitable material for biomedical applications such as targeted drug delivery systems or cancer treatment [9,10]. Moreover, the nanoparticles of PB/PBA are potential candidates for molecular sensors [11] or energy storage devices [12].

However, using the application potential of coordination systems requires some fabrication methodology of robust devices that can be handled and integrated without compromising functionality. One of the approaches allowing the achievement of this objective is the incorporation of the molecular system into the polymer matrix. The polymer matrix allows the development of different shapes, such as beads, spongy foam, membranes, and fibres. In the literature, one can find several examples of composite materials based on PBAs and organic polymers, such as collagen [13] or polyacrylonitrile [14]. These nanocomposites have received much attention as materials for radioactive Cs removal due to their affinity for adsorbing Cs^+ or microwave absorption.

Here, we report the preparation and characterization of the electrospun composites based on PVP and nanoparticles (NPs) of Prussian blue analogues. In the first stage of our work, we focused on the synthesis of the cyanido-bridged nanoparticles with narrow size distribution. Subsequently, the obtained nanoparticles were loaded into the polymeric matrix by use of electrospinning method. This straightforward technique enables the creation of fibres with diameters spanning from nano- to micrometres [15]. Its key benefits include cost-effectiveness, the capability to manufacture materials with a substantial surface area-to-volume ratio, and its adaptability

to various materials. Additionally, electrospinning offers the potential for integrating magnetic nanoparticles into electrospun fibre mats, maintaining both magnetic functionality and mechanical properties.

2. Material preparation and characterization

2.1. Materials

The following chemicals were purchased from Sigma-Aldrich without further purification: nickel(II) nitrate hexahydrate, trisodium citrate tetrahydrate, potassium hexacyanoferrate(III), potassium hexacyanochromate(III), poly(N-vinyl-2-pyrrolidone) (PVP) $M_w = 360\,000$ Da, and methanol.

2.2. Synthesis of PBA-NP NiHCM, M = [Fe, Cr]

In the following study, the literature protocol [16] for producing PBA nanoparticles in the presence of citrate anion was modified and used to produce two types of PBA NPs, i.e., nickel hexacyanoferrate (NiHCFe) and nickel hexacyanochromate (NiHCCr).

Nanoparticles of NiHCFe. In the first flask, 1.2 mmol of nickel(II) nitrate hexahydrate and 1.8 mmol of trisodium citrate tetrahydrate were dissolved in 40 ml of water. In the second flask, 0.8 mmol of potassium hexacyanoferrate(III) was dissolved in 40 ml of H_2O. After mixing both solutions, the mixture was left on magnetic stirring for 48 h at room temperature (20°C). The final product was separated from the supernatant by centrifugation at 9000 rpm for 15 min at a temperature of 10°C. The cleaning for the final product was as follows: a three-step washing procedure with distilled water and centrifugation at 9000 rpm for 15 min and at 10°C. The resulting orange solid was dried in a vacuum oven at 40°C for 20 h.

Nanoparticles of NiHCCr. The above synthetic protocol was repeated by substituting the source of cyanometallate for potassium hexacyanochromate(III). The precipitated material was washed with distilled water three times by centrifugation. The resulting light blue solid was dried in a vacuum oven at 40°C for 20 h.

2.3. Preparation of electrospun fibres

Composite fibres of NiHCM-PVP. The polymeric solution for electrospinning was prepared by introducing 43.00 mg of NiHCM (M = Fe, Cr) into 3 ml of MeOH. To ensure homogenous dispersion, the mixture was sonicated for 2 min without pulsation using an ultrasonic homogenizer.

Then, ~ 0.350 g of the PVP 360 powder was introduced to suspension to give a solution of 12 wt% PVP/MeOH+NiHCM and immediately put on the gyromixer for 3 h for the complete dissolution of polymer and to obtain a homogenous solution for electrospinning.

The polymer solution was inserted into the plastic syringe, from which it was electrospun with the homemade electrospinning equipment. During the process, the following conditions were applied: a voltage of 11 kV, room temperature (~ 20°C), relative humidity in the range of 46–52%, and constant flow rate of 1.5ml/h. The fibre mats were collected on a metallic plate collector randomly, with a distance between the tip and the collector equal to 10.5 cm.

2.4. Physical methods

Microstructure and composition analysis of films was performed using a TESCAN VEGA3 scanning electron microscope equipped with an X-ray energy dispersive spectrometer EDAX Bruker. For imaging under the electron microscope, small amounts of the freshly prepared NiHCFe and NiHCCr nanoparticles were dispersed by sonication in MeOH in order to obtain highly diluted solutions. The material was then transferred into the freshly cleaned Si (100) wafer by drop-casting and put aside for the solvent to evaporate. In the case of composite materials, they were directly electrospun onto the Si (100) wafers in small amounts to minimize the charging effects during imaging. The size of the particles and the diameters of the fibres were measured with the use of ImageJ software. The average sizes were calculated based on the lognormal distribution.

Powder X-ray diffraction (PXRD) data of nanoparticles and composites were collected on a PANalytical X'Pert PRO diffractometer equipped with a Cu K_α radiation source. The measurements were done using the Bragg–Brentano geometry. The diffraction patterns were indexed to determine the space group, and the lattice parameters were determined by doing a full-pattern Le Bail fit using the Mag2Pol software [17]. The indexing tool in Mag2Pol uses instrument geometry and the observed peak positions in a powder pattern and is based on the successive dichotomy method [18].

Raman measurements were performed using a confocal micro-Raman spectrometer (Nicolet Almega XR) equipped with a 532 nm laser. For powdered NiHCFe/NiHCCr, the measurement was performed with 1% of laser power to minimize the burning of the samples. NiHCM/PVP composites were directly electrospun onto the Si (100) wafers in small amounts, similar to preparation for scanning electron microscope (SEM) imaging. The measurements of composites were performed with 10% of laser power.
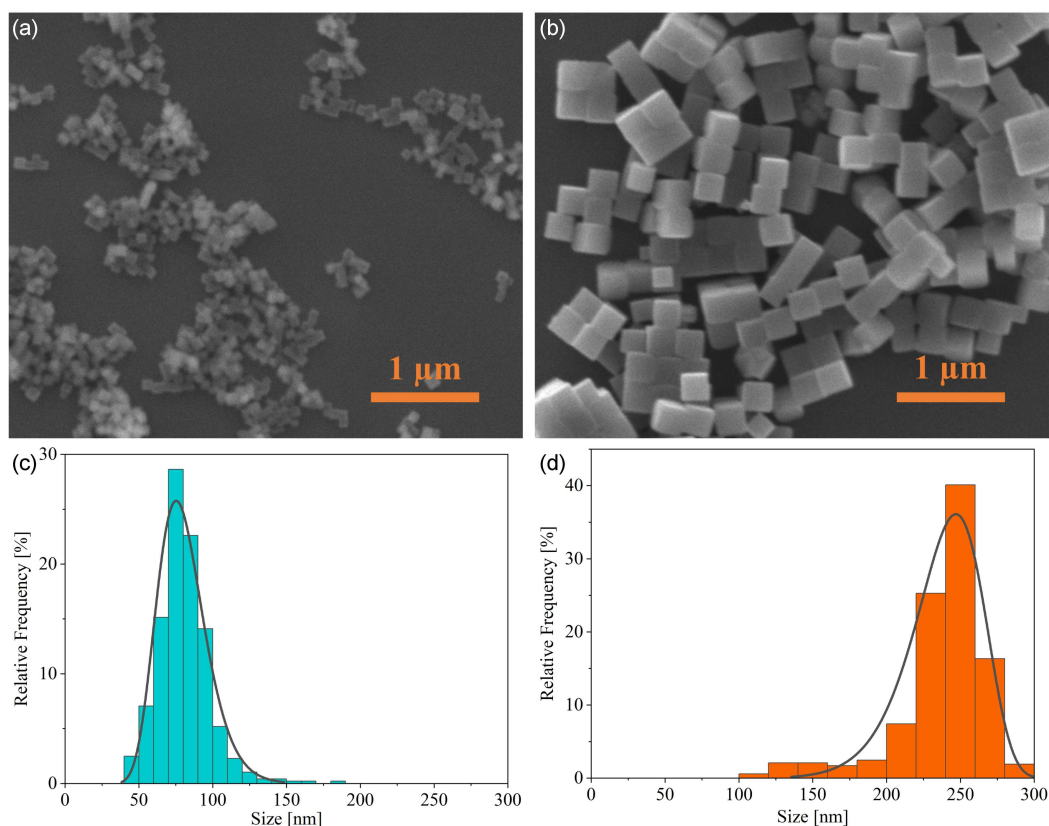
Fig. 1. (a, c) SEM image of NiHCCr NP, with lognormal distribution curve; (b, d) SEM image of NiHCFe NP, with Weibull distribution curve.
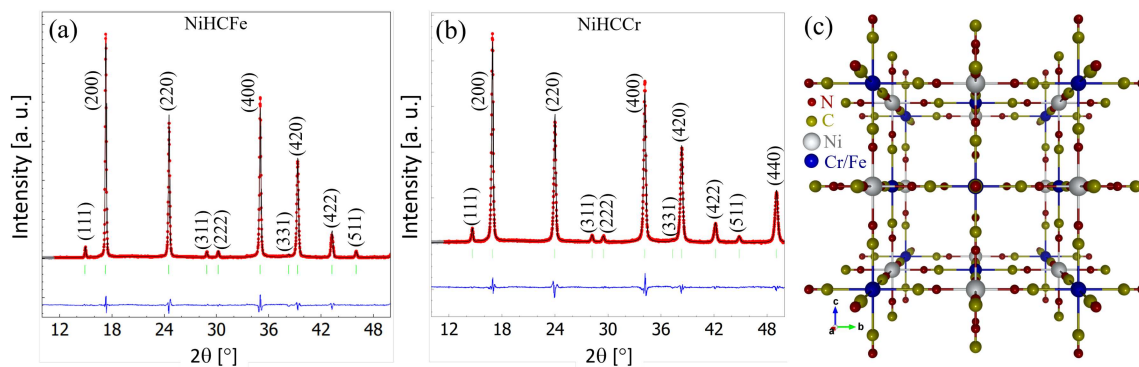

Fig. 2. X-ray diffraction data of (a) NiHCFe and (b) NiHCCr. The red circles are the experimental data, and the black curve is the profile calculated using the Le Bail method. Vertical bars indicate the expected Bragg positions, which are indexed and shown above. (c) A perspective view of NiHC(Fe/Cr) framework structure in a cubic Fm-$3m$ space group.

3. Results and discussion

PBA nanoparticles obtained in the synthetic protocol utilizing trisodium citrate salts as a size-tuning agent resulted in uniform, cubic-shaped particles presented in Fig. 1a and b. The size dispersion of cube diameter (Fig. 1c and d) showed that, despite the same synthetic protocol, the average diameter of the NiHCFe cubes (238 ± 37 nm) was three times bigger than for NiHCCr (80 ± 17 nm).

All the observed peaks of PXRD patterns of both samples were indexed with the cubic space group Fm-$3m$. No discernible impurity peaks were found in either compound. From the full-pattern Le Bail fit, the cubic unit cell parameter for NiHCFe and NiHCCr is found to be 10.2294(4) Å and 10.5016(6) Å, respectively. The Le Bail fit results of NiHCFe and NiHCCr are presented in Fig. 2a and b, respectively. Figure 2c shows a perspective view of the cubic lattice of the NiHC(Fe/Cr) framework.
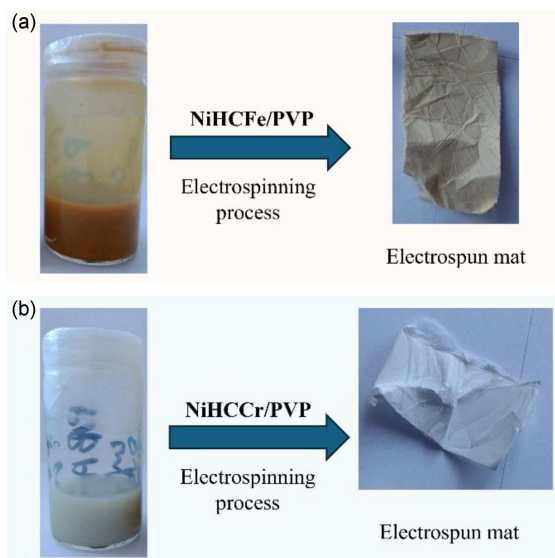
Fig. 3. Photographs of the polymer solutions prepared for the electrospinning process and the obtained electrospun mats.
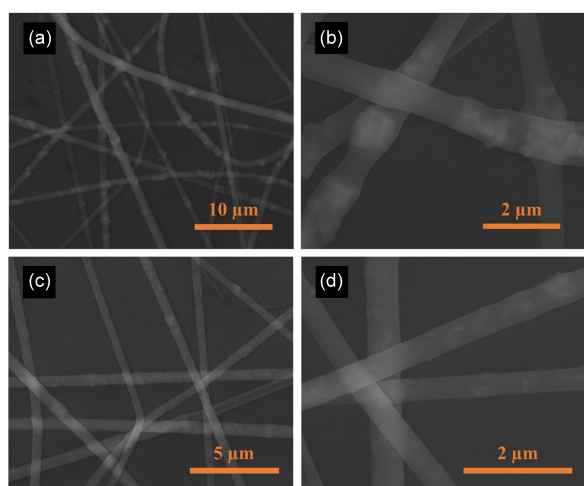

Fig. 4. The SEM pictures of the electrospun PVP nanofibres doped by NiHCFe (a, b) and NiHCCr (c, d) particles.

Fig. 5. Elemental mapping of PVP nanofibres loaded with 12 wt.% NiHCCr (a) and NiHCFe (b) nanoparticles by EDS.

In the preparation of composite materials containing PBA nanocubes in the form of electrospun fibres, it was necessary to carefully choose the polymer matrix as well as the solvent for the electrospinning solution. In this manner, poly(N-vinyl-2-pyrrolidone) (PVP) was chosen with the average molecular weight $M_n = 360$ kDa. It was selected due to its chemical stability and non-toxicity, as well as its widely used application as a stabilizing and capping agent in the synthesis of PB-type nanoparticles [19]. Methanol, in which PVP fully dissolves, was used as a solvent. In the first step of preparation of the solution for electrospinning, it was necessary to ensure a homogenous suspension of NiHCM nanocubes. For this reason, the mixture of freshly synthesized and dried PBA nanocubes was
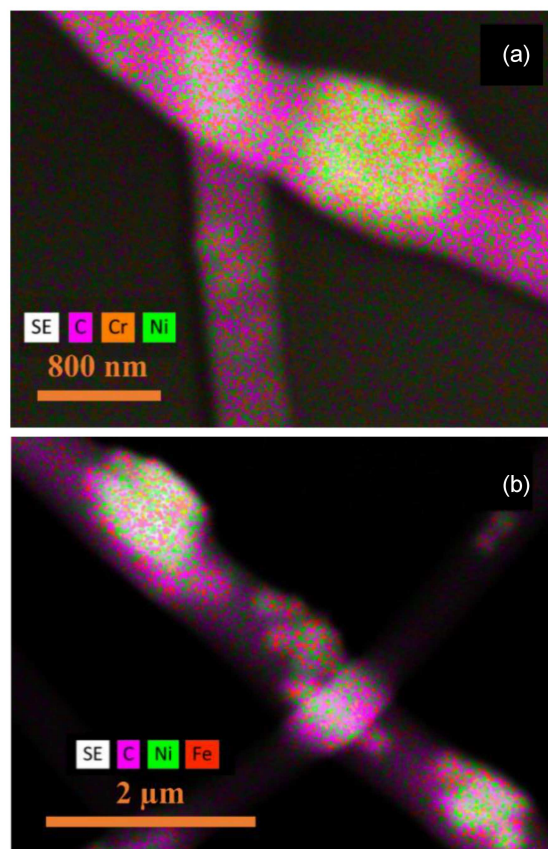
redispersed in an appropriate amount of methanol with the use of an ultrasonic homogenizer. After the procedure, the formation of aggregates in the suspension was not observed. Introducing adequate amounts of PVP 360 to form a 12 wt% polymer solution and allowing for the full dissolution of the polymer resulted in a solution ready for the electrospinning process (Fig. 3).

The electrospinning process of as-prepared PVP-based solutions with the initial concentration of NiHCM in composites equal to 12 wt% resulted in materials of two distinctive colours following the starting solutions — light orange and white, respectively for NiHCFe and NiHCCr (Fig. 3). The observation of freshly deposited electrospun fibres on a silicon wafer under SEM imaging presented in Fig. 4 showed differences in both materials due to the different dimensions of NiHCFe and NiHCCr nanocubes. For the NiHCFe/PVP material, the diameter of the PVP fibres was equal to 0.69 ± 0.15 μm, whereas the diameter of the thickened fragments resulting from nanocubes incorporation was equal to 0.97 ± 0.18 μm. In the case of the NiHCCr/PVP composites, the average PVP diameter is slightly diminished to 0.56 ± 0.12 μm, and the areas of the nanocubes aggregation resulted in the fibres thickening up
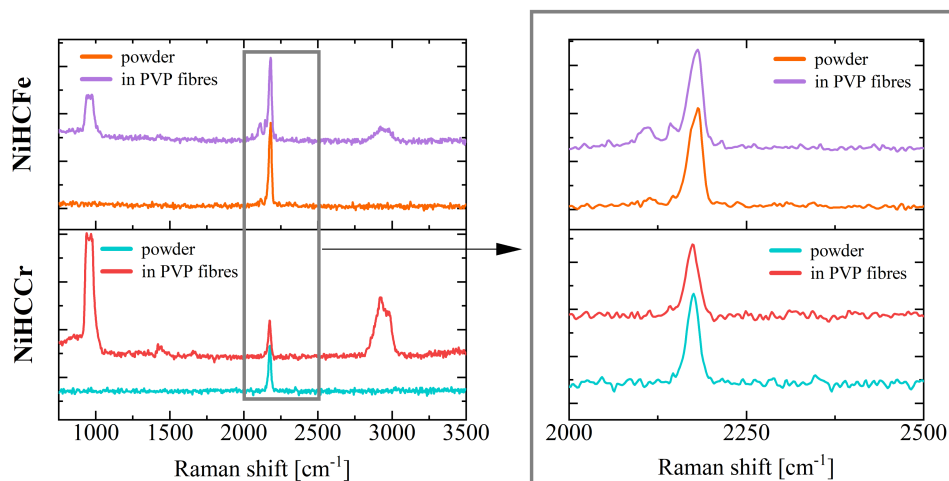
Fig. 6. Raman spectra of composite fibres of NiHCM-PVP and NiHCM bulk sample. On the right: enlargement of Raman spectra in the ν(CN) region.
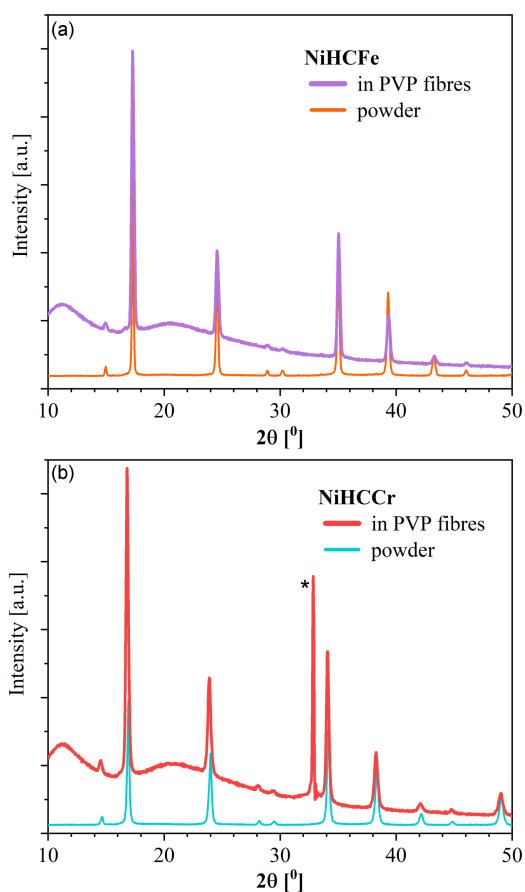

Fig. 7. The XRD pattern measured for composite fibres of NiHCM-PVP and NiHCM bulk sample.

originate from the incorporated nanocubes. Moreover, the incorporation of the cubical particles does not disrupt the structure of the fibre, as their dimensions are much smaller than fibre diameters. For both types of materials, the distribution of the nanocubes along the fibres is not perfectly homogenous, however, the diminished size of NiHCCr allows for noticeably better fibre morphology, which may have repercussions on the mechanical properties of the composite materials.

Raman spectroscopy was employed to investigate the composition of obtained materials. As depicted in Fig. 6, the Raman spectra of NiHCCr exhibited one prominent peak concentrated at 2175 cm^{-1}, corresponding to the CN vibrations of Cr^{III}–C≡ N–Ni^{II}. On the other hand, the Raman spectra obtained for NiHCFe exhibited one predominant peak at 2180 cm^{-1} originating from the CN vibration in Fe^{III}–C≡ N–Ni^{II} and two additional bands centred at 2145 cm^{-1} and 2110 cm^{-1}. The presence of these weaker bands reveals a partial reduction of Fe and indicates the appearance of Fe^{2+} in the samples. The appearance of the band corresponding to the CN vibrations in the Raman spectra registered for composite material confirms the effective incorporation of PBA nanoparticles into electrospun fibres.

Figure 7 shows the comparison of the X-ray diffraction (XRD) patterns of PVP and composites. XRD pattern of PVP confirms the amorphous nature of this polymer, where two distinct diffraction peaks were identified within the 10–15 and 15–24 ranges. These peaks might be associated with the two chain length and orientation, giving rise to the existence of two distinct amorphous phases of PVP. This observation aligns with existing literature [20, 21]. The XRD pattern of NiHCFe/PVP and NiHCCr/PVP composites exhibits peaks from both components, suggesting a successful blending of the two materials. The good quality of the

to 0.70 ± 0.14 μm. The broadening effect of the PVP fibre diameters is up to 40% and 25%, respectively, for the NiHCFe/PVP and NiHCCr/PVP composites. Energy dispersive X-ray spectroscopy (EDS) mapping of the thickened fragments of the fibres presented in Fig. 5 confirmed that they

obtained data also suggests a relatively high loading of the PBA-type nanocubes into the PVP fibres, observed in the distinctive colours of the electrospun mats (Fig. 3). The additional peak in the XRD pattern of NiHCCr/PVP marked by a star comes from the silicon background.

4. Conclusions

Two types of Prussian blue analogue (PBA) nanoparticles, namely nickel hexacyanoferrate (NiHCFe) and nickel hexacyanochromate (NiHCCr), were synthesized by the citrate-assisted co-precipitation method. The SEM images showed uniform and cubic-shaped particles for both types of nanoparticles. The electrospun fibres exhibited distinctive colours based on the type of PBA nanoparticles used. The mats were characterized using a scanning electron microscope (SEM), X-ray energy dispersive spectrometer (EDS), powder X-ray diffraction (PXRD), and Raman spectroscopy. The fibre morphology reveals differences between NiHCFe/PVP and NiHCCr/PVP composites, namely the incorporation of NiHCFe into PVP fibres brings about an increase in fibre diameter. EDS mapping confirmed the incorporation of nanocubes in the fibres without disrupting their structure. These results suggest the successful synthesis and characterization of PBA nanoparticles and their incorporation into composite fibres, paving the way for potential applications in various fields.

References

[1] L. Catala, T. Mallah, *Coord. Chem Rev.* **346**, 32 (2017).

[2] S. Ferlay, T. Mallah, R. Ouahès, P. Veillet, M. Verdaguer, *Nature* **378**, 701 (1995).

[3] W.R. Entley, G.S. Girolami, *Science* **268**, 397 (1979).

[4] S. Margadonna, K. Prassides, A.N. Fitch, *J. Am. Chem. Soc.* **126**, 15390 (2004).

[5] K.R. Dunbar, R.A. Heintz, *Chemistry of Transition Metal Cyanide Compounds: Modern Perspectives*, 1996, p. 283.

[6] J. Milon, M.-C. Daniel, A. Kaiba, P. Guionneau, S. Brandès, J.-P. Sutter, *J. Am. Chem. Soc.* **129**, 13872 (2007).

[7] S.S. Kaye, J.R. Long, *J. Am. Chem. Soc.* **127**, 6506 (2005).

[8] O. Sato, T. Iyoda, A. Fujishima, K. Hashimoto, *Science* **271**, 49 (1996).

[9] S. Mukherjee, R. Kotcherlakota, S. Haque, S. Das, S. Nuthi, D. Bhattacharya, K. Madhusudana, S. Chakravarty, R. Sistla, C.R. Patra, *ACS Biomater. Sci. Eng.* **6**, 690 (2020).

[10] C.R. Patra, *Nanomedicine* **11**, 569 (2016).

[11] R. Koncki, *Crit. Rev. Anal. Chem.* **32**, 79 (2002).

[12] B. Wang, Y. Han, X. Wang, N. Bahlawane, H. Pan, M. Yan, Y. Jiang, *IScience* **3**, 110 (2018).

[13] L. Peng, L. Guo, J. Li, W. Zhang, B. Shi, X. Liao, *Sep. Purif. Technol.* **307**, 122858 (2023).

[14] F. Chen, S. Zhang, R. Guo, B. Ma, Y. Xiong, H. Luo, Y. Cheng, X. Wang, R. Gong, *Compos. B Eng.* **224**, 109161 (2021).

[15] J. Xue, T. Wu, Y. Dai, Y. Xia, *Chem. Rev.* **119**, 5298 (2019).

[16] S. Keßler, G. González-Rubio, E.R. Reinalter, M. Kovermann, H. Cölfen, *Chem. Commun.* **56**, 14439 (2020).

[17] N. Qureshi, *J. Appl. Crystallogr.* **52**, 175 (2019).

[18] A. Boultif, D. Louër, *J. Appl. Crystallogr.* **37**, 724 (2004).

[19] T. Uemura, S. Kitagawa, *J. Am. Chem. Soc.* **125**, 7814 (2003).

[20] M.A. Ahmed, R.M. Khafagy, S.T. Bishay, N.M. Saleh, *J. Alloys Compd.* **578**, 121 (2013).

[21] M.T. Razzak, Zainuddin, Erizal, S.P. Dewi, H. Lely, E. Taty, Sukirno, *Radiat. Phys. Chem.* **55**, 153 (1999).